A Wide Charging Range Wireless Power Transfer Control System With Harmonic Current to Estimate the Coupling Coefficient

Jianghao Hu, Jiankang Zhao, and Chao Cui

***Abstract*—In the wireless power transfer (WPT) control system, estimating the coupling coefficient (k) is an essential step to achieving optimal control over a wide charging range. The estimate required signal of the traditional WPT system is mainly the currentand voltage generated by fundamental. It requires many parameters and complex calculations to estimate k by analyzing these electrical signals, which makes the traditional method of estimating k difficult to achieve good robustness and application in practice. To reduce the process of estimation, a method of estimating k only by the harmonic current is proposed in this article. According to this method, a wide charging range WPT control system is designed. The main feature of the control system is that it is very easy to estimate k because the high frequency harmonic can simplify the circuit. By analyzing the system characteristics under different harmonic currents, the system can achieve optimal control over a wider charging range. In addition, a WPT system that meets the Qi standard is designed and tested. The experimental results show that the original 10 mm Qi standard charging distance can reach 20 mm.**

***Index Terms*—Coupling coefficient estimation, harmonic currents, optimal control, wide charging range, wireless power transfer (WPT).**

I. Introduction

WIRELESS power transmission (WPT), which originated more than 100 years ago, has been successfully applied in many areas [1], including mobile phones, automobiles, medical electronics, etc. WPT has a promising future, but there are still many technologies that need to be improved for the further development of WPT, including system control [2]–[4], system efficiency [5], charging distance, foreign object detection, electromagnetic interference [6], etc.

Most WPT systems use a bridge inverter, whose output voltage is a square wave that contains many high frequency harmonics. Using harmonic to transmit power is an interesting research area. A WPT system with selected harmonic resonance has been proposed to design smaller and lighter coils [7]. A design consideration on the usage of harmonic currents for PHEV and EV charger and a comprehensive comparison between different harmonic orders as the power carrier have been proposed [8]. Different from the study of the harmonic as the power carrier, this article mainly takes the harmonic as the information carrier, thus proposing the relationship between the harmonic and coupling coefficient k as well as further using this relationship to design a wide charging range WPT control system.

The k represents the relationship between the position of the receiving coil and the transmitting coil, which is difficult to measure directly, and k affects all of the characteristics of WPT system; therefore, it is very important to estimate k. The traditional method of estimating k is mainly to measure and calculate the electrical signal generated by the fundamental [9]–[18]. In this article, the traditional methods are divided into the following two types according to the measurement position of the electrical signal.

1) *Estimate k by the Electrical Signal of the Transmitter:* Jang *et al.* [9] proposed a one-port measurement method to estimate the k in frequency-tuned WPT systems. A front-end monitoring method of a WPT system without the requirement of measurements on the receiver circuit is presented [10]. Chow *et al.* [11] presented an investigation into the use of the transmitter-side electrical information to estimate the k. A method for estimating k without wireless communication is proposed [12].

2) *Estimate k by the Electrical Signal of the Receiver:* A calculation method is proposed using the primary voltage and the k on the secondary side to eliminate the need for the primary voltage regulation [13]. A method of k estimation with recursive least squares filter is proposed [14], [15]. An approximately real-time identification method of k is proposed to help achieve the current maximum efficiency in a nonideal system [16].

There is a method to estimate k by measuring the electrical signals at both ends, which can essentially belong to the second type because its measurement of the duty cycle can reflect the change in the electrical signals of the receiver [17]. At the same time, Jiwariyavej *et al.* [18] introduced both types of traditional methods and deduces the method of estimating the multicoil k.

The common feature of traditional methods is that the frequency of estimating k is fundamental. However, the characteristic of the WPT system under the fundamental frequency are nonlinear resonance, which has a very complex relationship with k. The estimation of k requires many parameters and complex calculation, which leads to the lack of robustness and practical

Manuscript received May 26, 2020; revised August 24, 2020; accepted October 6, 2020. Date of publication October 21, 2020; date of current version January 22, 2021. Recommended for publication by Associate Editor R. Zane. *(Corresponding author: Jiankang Zhao.)*

The authors are with the Department of Instrument Science and Engineering, Shanghai Jiao Tong University, Shanghai 200240, China (e-mail: jianghaohu@outlook.com; 404225202@qq.com; tsuibeyond@sjtu.edu.cn).

Color versions of one or more of the figures in this article are available online at https://ieeexplore.ieee.org.

Digital Object Identifier 10.1109/TPEL.2020.3032659

application. Jiwariyavej *et al.* [18] experiment also confirmed that the estimation of *k* near the fundamental frequency requires high measurement accuracy, and the variation of parameters will lead to a large deviation in the result. To reduce the process of estimation, this article proposes a method of estimating *k* only by the harmonic current. In this method, the circuit is simplified by high frequency harmonic to reduce the complexity of *k* estimation, and the reduction of calculation parameters also improves the robustness of this method. To show the contribution of this method more intuitively, Tables I and II summarize the methods for estimating *k* and focus on the differences in complexity and robustness.

Currently, the mainstream standard of the WPT is the Qi standard defined by the wireless power consortium [19]. The Qi is the first WPT standard, and most mobile phone products are based on it. The electrical signal of the Qi standard is the current and voltage generated by the fundamental, and thus, it is difficult to estimate the specific *k* of the system to achieving optimal control over a wide charging range. In order to solve this problem, a wide charging range WPT control system is designed. The main feature of the control system is that it is very easy to estimate *k* because the high frequency harmonic can simplify the circuit. By analyzing the system characteristics under different harmonic currents, the system can achieve optimal control over a wider charging range. In addition, a WPT system that meets the Qi standard is designed and tested. The experimental results prove that the original 10 mm Qi standard charging distance can reach 20 mm.

The rest of this article is organized as follows. Section II will introduce the principle of estimating *k*, including the traditional method and the method proposed in this article. In Section III, the system characteristics and control methods under different coupling are deduced through modeling and analysis. Section IV mainly introduces the experiments and results of the system under the Qi standard. Finally, Section V concludes the article.

II. Principle of Estimating the Coupling Coefficient

This section mainly introduces the principle of estimating *k*, including the traditional method and the method proposed in this article. The inverter output voltage of the WPT system is generally a square wave, which can be decomposed into the fundamental and harmonics by Fourier. When the fundamental and harmonic are input into WPT system, the corresponding electrical signal will be generated on the circuit. The measurement and calculation of these electrical signals is a necessary step to estimate *k*, in which only measuring the harmonic signal is the main difference between the traditional method and the proposed method. Fig. 1 shows the frequency source of the electrical signal required for *k* estimation, in which C_P is the resonance capacitance of the transmitter, r_p is the equivalent resistance of the transmitter, L_P is the transmitting coil, and L_S is the receiving coil.

A. Principle of Estimating the Coupling Coefficient by the Traditional Method

According to the measurement position of the electrical signal, the traditional method can be divided into two types:

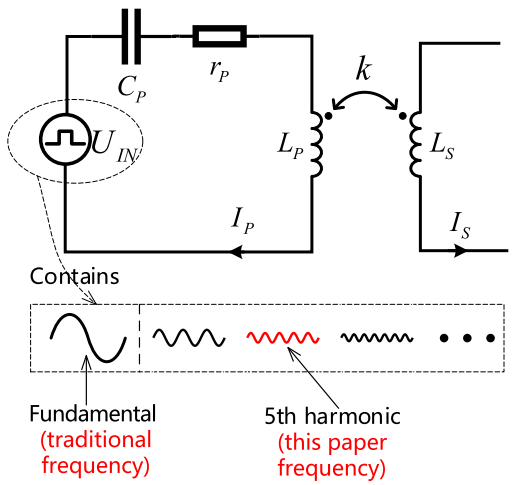

Fig. 1. Frequency source of the electrical signal required for *k* estimation.

transmitter electrical signal to estimate *k* and receiver electrical signal to estimate *k*. In this section, the principles of these two types will be introduced.

1) *Estimate k by the Electrical Signal of the Transmitter:* The input current will be generated when the fundamental is input into the transmitter. The amplitude I_P and phase $\angle\theta_{Ip}$ of the input current are affected by *k*. It is a general method to estimate *k* by measuring the I_P and $\angle\theta_{Ip}$. The formula for the estimation of *k* is as follows [10]:

(All of the formula symbols quoted in this article are unified according to Fig. 1)

$$k = \sqrt{\frac{\frac{1}{\omega L_P} - \frac{1}{\omega^3 L_P L_S C_S}}{\mathrm{Im}\left[\left(\frac{U_{\mathrm{IN}}}{I_P}\right)\angle\theta_{Ip} - r_p - j\omega L_P - j\left(\frac{1}{\omega C_P}\right)\right]^{-1}}}. \quad (1)$$

It can be seen from the abovementioned formula that the estimation of *k* is based on the calculation of the I_P and $\angle\theta_{Ip}$. There are two limitations to this method. The first is that the derivation of the formula is based on the resistive load. If the load is capacitive or inductive, the formula is not valid. The second is that if the frequency is equal to the resonance frequency, the formula denominator will be zero.

Formula (1) is solved by the phasor method, and *k* can also be estimated by the time-domain method. To estimate *k* by the time-domain method, two instantaneous values of the input current $i_{p(a)}$ and $i_{p(b)}$, and the corresponding instantaneous values of input voltage $\upsilon_{\mathrm{in}(a)}$ and $\upsilon_{\mathrm{in}(b)}$ need to be measured. The formula for estimating *k* by the time-domain method is as follows [11]:

$$k = \frac{\left[\upsilon_{Lp}(\omega t) + \upsilon_{Cp}(\omega t) + i_p(\omega t)\, r_p - \upsilon_{in}(\omega t)\right] d\omega t}{\omega\sqrt{L_P L_S}\, di_S(\omega t)}. \quad (2)$$

Compared with the phasor method, the time-domain method has no limitation. The essence of time-domain is the same as the phasor method, that is, two kinds of mathematical tools. The main disadvantage of the time-domain method is that the amount of calculations is too large, and the current distortion caused by the diode needs to be calculated, otherwise the accuracy of the result will be affected.

TABLE I
COMPLEXITY COMPARISON BETWEEN THE TRADITIONAL METHOD AND THE METHOD IN THIS ARTICLE

Electrical signal position	Electrical signal required	circuit parameters required	Number of linear calculations	Number of nonlinear calculations	Paper sources
Transmitter	I_P $\angle\theta_{Ip}$	U_{IN}, L_P, C_P, r_p ω, L_S, C_S, r_s	14	4	**[10]**
Transmitter	$\upsilon_{in(a)}$, $\upsilon_{in(b)}$ $i_{p(a)}$, $i_{p(b)}$	L_P, C_P, r_p L_S, C_S, r_s	>20	>10	**[11]**
Transmitter	$I_{P(peak)}$ $I_{P(WR-)}$, $I_{P(WR+)}$	U_{IN}, L_P C_P, r_p	>20	>10	**[9]**
Transmitter	I_P, $I_{P_{(3rd)}}$ $\angle\theta_{Ip_{(3rd)}}$	U_{IN}, L_P, C_P, r_p ω, L_S, C_S	>20	>10	**[12]**
Receiver	U_S I_S	U_{IN}, L_P, r_p ω, L_S, r_s	12	4	**[13]-[16]**
Transmitter and Receiver	ΔD R_L	U_{IN}, L_P, r_p ω, L_S, r_s	>20	>10	**[17]**
Transmitter	$I_{P(5th)}$	U_{IN}, L_P, ω	**5**	**1**	**This paper**

It is a feasible method to estimate *k* by the frequency splitting characteristic of the system [9]. When *k* is greater than a specific value, there will be frequency splitting, and then, the I_P will have two peaks. By measuring these two peaks, *k* can be estimated. The disadvantage of this method is the difficulty and accuracy of measurement. *k* can also be estimated by the comprehensive calculation of the fundamental and harmonic electrical signals at the transmitter [12]. In this method, *k* is calculated by I_P, the amplitude of third harmonic current $I_{P(3rd)}$ and the phase $\angle\theta_{Ip(3rd)}$. Although harmonics are used in this method and the proposed method, the two methods are different in essence. Harmonic current of this method is one of the required electrical signal, not the only one. This method is still mainly calculated under fundamental frequency.

2) *Estimate k by the Electrical Signal of the Receiver:* Similar to the previous analysis, the input fundamental will also generate many electrical signals in the receiver, and *k* can also be estimated through the measurement and calculation of these electrical signals. It is a very general method to estimate *k* by measuring the output current I_S and output voltage U_S of the receiver, and its formula is as follows [13]–[16]:

$$k = \frac{U_{\text{IN}} \pm \sqrt{U_{\text{IN}}^2 - 4 r_p I_S \left(U_S + r_S I_S\right)}}{2\omega I_S \sqrt{L_P L_S}}. \tag{3}$$

It can be seen from the above formula that there will be two results, which requires some logical judgment to obtain the real value. Table I adds these logical judgments to the number of nonlinear calculations. The disadvantage of this method is that it is not suitable for the optimal control system without communication module.

In addition to the method of formula (3), the receiver electrical signal estimating *k* can also use the phasor, time domain, and other methods, which is similar to the transmitter estimating *k*. The method by measuring the duty cycle is essentially the same as that of the receiver electrical signal [17]. In this method, the change in the receiver's electrical signal is reflected by the change in the duty cycle of the dc–dc. The disadvantage of this method is that the number of calculations is very large. At the same time, it can only be used in a circuit system where both the transmitter and the receiver have dc–dc modules.

B. Principle of Estimating the Coupling Coefficient Only by the Harmonic Current

The WPT resonant circuit is composed of inductance and capacitance, which have different reactance at different frequencies. There is little difference in the reactance of these components under the fundamental frequency, and thus, all components need to participate in the calculation, which is the reason why the estimation of *k* under the fundamental frequency is complex. The reactance of the inductance and capacitance will change greatly under high frequency harmonic. The inductance is nine times the reactance of the capacitance in the third harmonic and 25 times that in the fifth harmonic. Due to the large difference in component values, some components do not participate in the calculation and will not affect the results, and thus, the WPT circuit can be simplified under the high frequency harmonic, and the number of electrical signals and calculations required will be greatly reduced after the simplification, which is the reason why the estimation of *k* under the harmonic frequency is simple.

The simplified circuit of series-parallel topology (SP) at high frequency is shown in Fig. 2. The capacitance and equivalent resistance under the high frequency harmonic can be ignored because they are far less than the inductance. Similarly, the load R_L of the SP can also be ignored because R_L is parallel to the capacitance, which is nearly short circuited at high frequency. After the simplification of the circuit, only two electric signals are left: the transmitter harmonic current signal $I_{P,n}$ and the receiver harmonic current signal $I_{S,n}$. Their relationship with *k* is as follows:

$$I_{P,n(\text{simplified})} = \frac{U_{\text{IN},n}}{\left(1 - k^2\right) j\omega_n L_P} \tag{4}$$

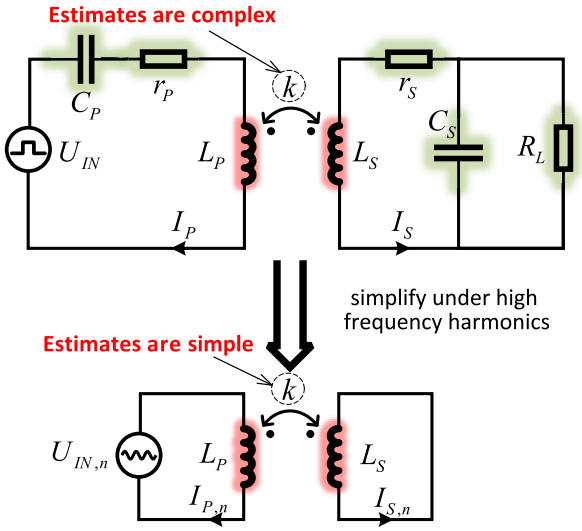

Fig. 2. WPT circuit simplification under high frequency harmonic. *(Main principles of the proposed method.)*

$$I_{S,n(\text{simplified})} = \frac{U_{\text{IN},n}}{(1\ k-k)\, j\omega_n \sqrt{L_P L_S}} \tag{5}$$

where $U_{\text{IN},n}$ is the nth harmonic input voltage ($U_{\text{IN},n} = U_{\text{IN}}\ n$) and ω_n is the nth harmonic angular frequency ($\omega_n = n\omega$). In this article, the input voltage U_{IN} is defined as the amplitude of a phasor. If the input voltage is described as a time-domain square wave, then its Fourier amplitude is $4U_{\text{IN,dc}} \sin(n\pi\ 2)\ (n\pi)$.

Through the analysis of the abovementioned two formulas, it can be found that the sensitivity of $I_{P,n}$ is higher when the k is high (the closer k is to 1, the greater the change in $I_{P,n}$ is), while the sensitivity of $I_{S,n}$ is higher when the k is low (the closer k is to 0, the greater the change in $I_{S,n}$ is). Therefore, the type of harmonic current signal can be selected according to the sensitivity needs. Since the formula (4) does not need L_S to participate in the calculation, $I_{P,n}$ is used as the harmonic signal to estimate k in this article.

The simplified circuit with the higher order harmonic is more accurate than that with the lower order harmonic. To further research the relationship between the harmonic order and the result, we have listed the formula of the relationship between the $I_{P,n}$ and k before simplification as follows:

$$I_{P,n(\text{complete})} = \frac{U_{\text{IN},n}}{\frac{1}{j\omega_n C_P} + r_P + j\omega_n L_P + Z_r} \tag{6}$$

where

$$Z_r = \frac{k^2\omega_n^2 L_P L_S}{r_S + j\omega_n L_S + \frac{1}{j\omega_n C_S} // R_L}.$$

Through the simulation of formulas (4) and (6) under different orders, Fig. 3, can be drawn. The range of k is defined between 0 and 0.9 in this article because when k exceeds 0.9, $I_{P,n}$ changes too much for convenient analysis. At the same time, the magnetic coupling path of WPT is air, and thus, it is difficult for k to exceed 0.9. We can obtain the accuracy by calculating the results of each order. This accuracy is defined

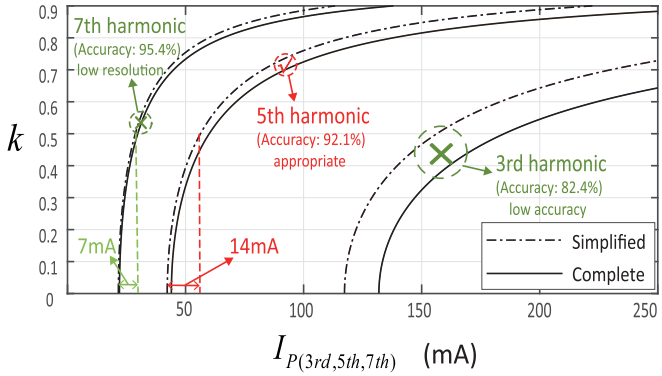

Fig. 3. Accuracy comparison of different harmonic orders after the simplification ($L_P = 7.4\,\mu H$, $L_S = 25\,\mu H$, $C_P = 330\,nF$, $C_S = 47\,nF$, $r_p = 0.5\,\Omega$, $r_s = 0.5\,\Omega$).

as $|(I_{P,n(\text{complete})} - I_{P,n(\text{simplified})})\ I_{P,n(\text{complete})}| \times 100\%$. The accuracy of the third harmonic is 82.2%, that of the fifth is 92%, and that of the seventh is 95.4%. The accuracy increases with the increase in the order. This is because with the increase in the order, the frequency is also increasing, which leads to the simplified value being closer to the real value. However, too high of a order will cause low $I_{P,n}$ resolution, i.e., the change of harmonic current in low coupling is very small. When $k \in (0, 0.5)$, the change value of fifth harmonic current is 14 mA, and that of the seventh is reduced to 7 mA. The low resolution makes it difficult to get the specific coupling coefficient under the low coupling. Therefore, the order needs to be determined by both resolution and accuracy. In this article, the accuracy of the fifth harmonic can meet the control requirements, and the resolution is not low, so the fifth harmonic order is taken as the selected order.

By changing formula (4), we can obtain the expression of the harmonic to estimate k as follows:

$$k = \sqrt{1 - \frac{U_{\text{IN}}}{25 * I_{P(5th)} j\omega L_P}}. \tag{7}$$

By comparing formula (7) with formulas (1) and (3), it can be found that for the method in this article, only one electrical signal $I_{P(5th)}$ and three circuit parameters $U_{\text{IN},n}$, ω and L_P are needed to estimate k, which greatly reduces the calculation process. Table Iis a comparison of the calculation amount between the traditional method and the method proposed in this article, in which the nonlinear calculation also includes the logic judgment.

The circuit parameters in Table I are the characteristic parameters of the system itself, which are defined as quantitation in the formula for estimating k. If these quantitations change, it will cause deviation to the results. When the result deviation caused by quantitative change is smaller, it means that the robustness of the method is higher, otherwise it is not. The coil inductance is a kind of parameter that is easy to change because ferrite will be added to the back of the coil in many cases, which makes the transmitting coil and the receiving coil influence each other so the inductance will increase at a short distance. The resonance capacitance of the system is also affected by the aging of the

TABLE II
ROBUSTNESS COMPARISON BETWEEN THE TRADITIONAL METHOD AND THE METHOD IN THIS ARTICLE

Δk / $\Delta 10\%$	Traditional method (transmitter)	Traditional method (receiver)	**The method in this paper**
L_P	16.7%	14.9%	12.0%
C_P	3.8%	13.8%	**0.9%**
r_p	5.6%	5.6%	**0.1%**
L_S	7.6%	3.7%	**0.7%**
C_S	5.7%	3.4%	**0.5%**
r_s	0.1%	0.1%	**0.1%**

medium and the distributed capacitance in the environment. The internal resistance of the system is also affected by the skin effect and ambient temperature. Therefore, Table II is added in this article to compare the influence of 10% changes in inductance, capacitance and resistance on the accuracy of the results. The traditional method uses the most frequently used formulas (1) and (3), while the method in this article uses the more accurate formula (6).

It can be found from Table II that only L_P can make the result deviate in the method of this article because most circuit parameters can be ignored at high frequency, and thus, the changes in these parameters will not affect the result. Therefore, compared with the traditional method, this method not only greatly reduces the calculation but also has high robustness.

C. Application of the Proposed Method in Other Topologies

The abovementioned analysis is based on SP topology. This section will further analyze the application of the proposed method in SS, LCC, etc. The principle of the proposed method is to reduce the complexity of k estimation by simplifying the circuit through high frequency harmonic. The main way to simplify the circuit is to short circuit the capacitance at high frequency. At the same time, when the capacitance is in parallel, all the circuits in parallel can be short circuited, so the position of the capacitance determines the simplified result of the circuit.

Similar to the principle of Fig. 2, the simplification of different topologies under high frequency harmonic is shown in Fig. 4. It can be seen from Fig. 4, that for LCC–LCC, when there is a capacitance in parallel at the transmitter, the harmonic current will not flow through the coil, which means that it does not have the function of estimating k. Therefore, the proposed method is not suitable for the topology with parallel capacitances at the transmitter.

For SS and S-LCC, there is no parallel capacitance at the transmitter, so they can estimate k by harmonic current. Moreover, the receiver of S-LCC has a parallel capacitance, so its simplified circuit and k estimation process are the same as SP. However, the receiver of SS has no parallel capacitance, so its simplified circuit is a series circuit composed of receiving coil and load. If k needs to be estimated, the effect of load should be further considered.

If the load appear in the k estimation formula, this means both the transmitter and receiver signals are required, which

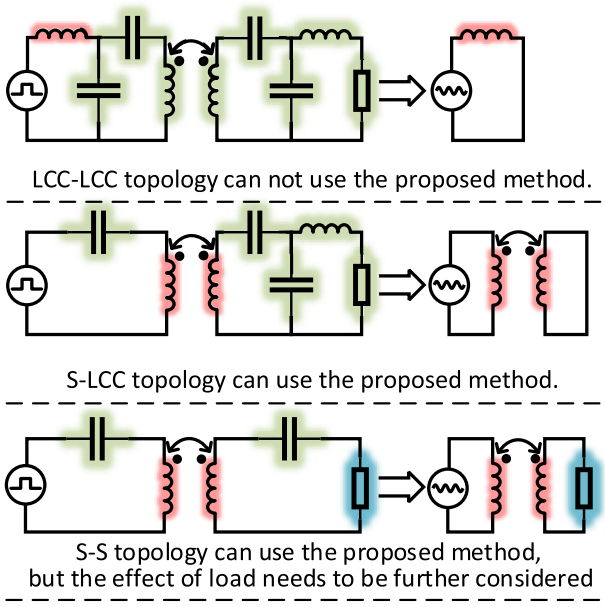

Fig. 4. Application of the proposed method in other topologies.

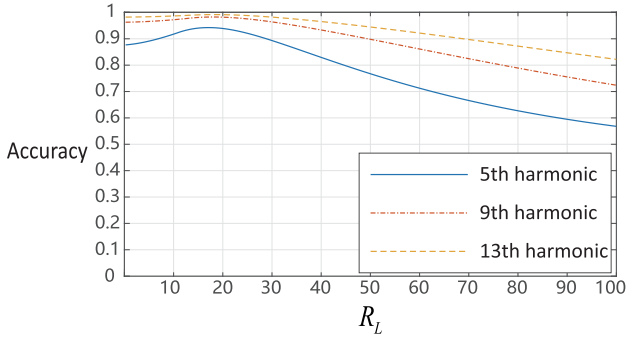

Fig. 5. Accuracy comparison of different orders and R_L in SS topology.

increases the complexity of estimating k. So this article continues to analyze how to simplify the load. The harmonic current with load in SS topology is as follows:

$$I_{P,n(SS,\text{simplified})} = \frac{U_{\text{IN},n}\left(1+\frac{R_L}{j\omega_n L_S}\right)}{(1-k^2)\,j\omega_n L_P + \frac{R_L L_P}{L_S}}. \tag{8}$$

By observing the abovementioned formula, it can be found that when the harmonic order is increased (ω_n increases), it is closer to formula (4). This is because when the coil reactance is much larger than R_L, ignoring R_L will not have a great impact on the harmonic current, so the influence of R_L can be ignored by increasing the order.

In order to analyze the relationship between orders and R_L more intuitively, Fig. 5 shows the change of result accuracy under different orders and R_L. The accuracy analysis object are complete harmonic current and simplified harmonic current without load. The results in the Fig. 5, further verify that the influence of R_L in SS topology can be ignored by increasing the order. Increasing the order will lead to the problem of low

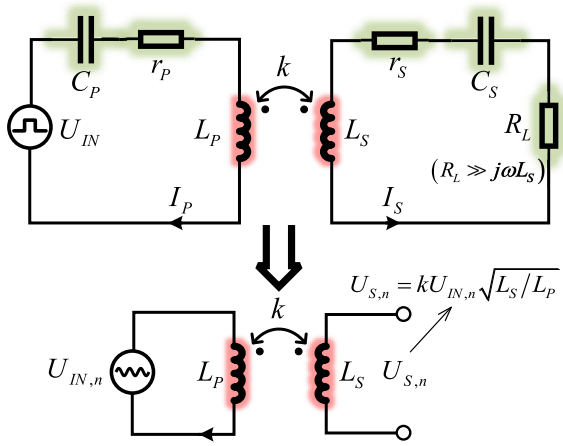

Fig. 6. SS topology estimates k by harmonic voltage of receiver. ($R_L \gg j\omega L_S$).

resolution under low coupling, which can be solved by replacing analysis $I_{P,n}$ with $I_{S,n}$. It is also observed that the accuracy is not the highest when R_L tends to zero. This is because when the load is too small, the effect of resonant capacitance and internal resistance on harmonic current will be greater.

It can also be seen from Fig. 5, that it is difficult to obtain ideal accuracy by increasing the order when R_L is large. In this case, k can also be estimated by reducing the order and analyzing the receiver harmonic voltage $U_{S,n}$. This method is contrary to the proposed method to estimate k by harmonic current at the transmitter. Its principle is shown in Fig. 6, R_L can be regarded as open circuit when $R_L \gg j\omega L_S$. At this time, the harmonic voltage on R_L is $kU_{\mathrm{IN},n}\sqrt{L_S\ L_P}$, which has a very single relationship with k.

In conclusion, there is no parallel capacitance at the transmitter, which is the basis condition for the proposed method to be used in topology. If there is no parallel capacitance in the receiver, the effect of R_L should be considered. When R_L is not large, the effect of R_L can be ignored by increasing the order. When R_L is large, we can reduce the order and analyze $U_{S,n}$ to estimate k.

III. Characteristic Analysis and Control Research of the System Under Different Coupling

A. Modeling and Analysis

The abovementioned section analyzes the principle and characteristics of the harmonic to estimate k, which has the advantages of simple calculation and high robustness compared with the traditional method. Based on this method, this article designs a control system with the harmonic current to estimate k. Its basic circuit topology is series parallel with switch buck (SP-BUCK), as shown in Fig. 7. This section mainly models and analyzes the circuit under coupling.

The reflected impedance is a good way to analyze the WPT system. When the WPT system is analyzed from the transmitter, the receiver is equivalent to a reflected impedance that is connected with the primary coil in series. The power consumed

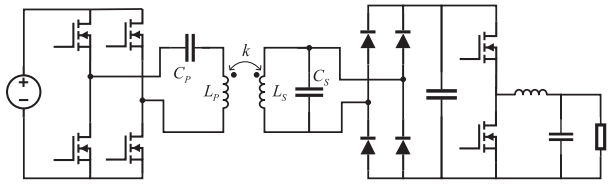

Fig. 7. Circuit topology.

by the reflected impedance is equivalent to the power that the receiver receives. The reflected impedance directly reflects the relationship between the transmitter and the receiver. The larger the reflected impedance is, the tighter the relationship is, the higher the efficiency is, and vice versa. The real part of the reflection impedance of SP is given as follows. The following formula ignores the coil resistance and assume $\omega = \omega_P$:

$$\mathrm{Re}Z_{r,sp} = \frac{k^2 L_P R_L}{L_S}. \tag{9}$$

The reflection impedance is positively correlated with the harmonic current. The larger the harmonic current is, the higher the k is, the greater the reflection impedance is.

Use formula (7) to obtain

$$\mathrm{Re}Z_{r,sp} = \left(1 - \frac{U_{\mathrm{IN}}}{25 * I_{P(5th)} j\omega L_P}\right)\frac{L_P R_L}{L_S}. \tag{10}$$

For an ideal buck converter, the input power is equal to the output power, and the output voltage is related to the input voltage and duty ratio. The correlation is shown as follows:

$$\frac{U_{\mathrm{in,buck}}^2}{R_{\mathrm{in,buck}}} = \frac{U_{\mathrm{out,buck}}^2}{R_{\mathrm{out,buck}}} \tag{11}$$

$$U_{\mathrm{out,buck}} = DU_{\mathrm{in,buck}} \tag{12}$$

where D is the duty cycle, $R_{\mathrm{in,buck}}$ is the input resistance, and $R_{\mathrm{out,buck}}$ is the output resistance of the buck converter. From the abovementioned two formulas, we can obtain the following formula:

$$R_{\mathrm{in,buck}} = \frac{R_{\mathrm{out,buck}\cdot}}{D^2} \tag{13}$$

The abovementioned formula shows that the buck converter has the function of amplifying the output resistance, and the magnification multiplier is 1 D^2 times. When the buck converter is combined with the SP circuit, the reflected impedance of the transmitter is magnified by 1 D^2 times, and the reflected impedance is changed to

$$\mathrm{Re}Z_{r,sp-\mathrm{buck}} = \left(1 - \frac{U_{\mathrm{IN}}}{25 * I_{P(5th)} j\omega L_P}\right)\frac{L_P R_L}{D^2 L_S}. \tag{14}$$

Fig. 8(a) shows the equivalent circuit of SP-BUCK, which adds a buck converter to the SP equivalent circuit. The circuit model of the buck converter is complex. The internal parameters include the input voltage, input current, control method, switching frequency, duty cycle, and so on [20]. To simplify the analysis, the buck converter is approximately equivalent to a dynamically tunable autotransformer T_{buck}. The efficiency of T_{buck} varies with the internal parameters. The relationship between the

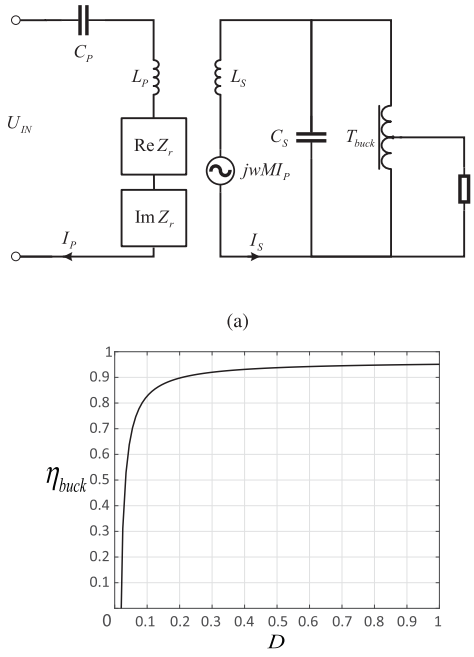

Fig. 8. (a) System equivalent circuit diagram. (b) Relationship between the efficiency and D in buck circuits. (Simulation based on the data provided by LM46002 manual, $\eta_{\text{buck}} = 0.96\text{-}0.013/D$.)

efficiency of buck η_{buck} and D is shown in Fig. 8,(b). From this figure, we can see that when D is very small, T_{buck}'s efficiency drops rapidly, which indicates that the load amplification cannot be too high.

By modeling the circuit, we find that when $\omega_S = \omega_P$ [ω_S=1 $(2\pi\sqrt{L_S C_S})$, ω_P=1 $(2\pi\sqrt{L_P C_P})$], the input of the system has capacitive reactance $\mathrm{Im}Z_r$ and imaginary part power, thus increasing the inverter loss and power loss. In addition, the capacitive reactance causes the input current phase to exceed the voltage phase, which leads to the switching loss of the MOSFET in the inverter rising rapidly, thus further reducing the system efficiency. To solve this problem, we can make $\omega_P < \omega_S$ so that the transmitter has inductive reactance to counteract the capacitive reactance.

According to formula (9), it can be observed that it has different reflection impedances under different *k*. We can obtain Fig. 9, by simulating the output power and efficiency under different *k*. The formula of system efficiency and output power is as follows:

$$\eta = \frac{\omega^2 k^2 L_P L_S \eta_{\text{buck}} R_L \ D^2}{\left[\omega^2 k^2 L_P L_S + \left(r_S + \frac{R_L}{D^2}\right) r_P\right]\left(\frac{R_L}{D^2} + r_S + \frac{r_S \omega^2 C_S^2 R_L^2}{D^4}\right)} \tag{15}$$

$$P = \frac{U_{\text{IN}}^2 \omega^2 k^2 L_P L_S \eta_{\text{buck}} R_L \ D^2}{\left|\left(Z_P Z_S + \omega^2 k^2 L_P L_S\right)^2 \left(\frac{\omega C_S R_L}{D^2} - j\right)^2\right|} \tag{16}$$

where

$$Z_P = r_P + j\omega L_P + 1 \ j\omega C_P$$

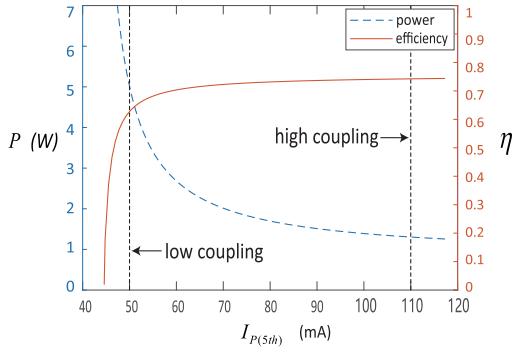

Fig. 9. Output power and efficiency under different *k*. ($L_P = 7.4\,\mu H$, $L_S = 25\,\mu H$, $C_P = 330\,nF$, $C_S = 47\,nF$, $r_p = 0.5\,\Omega$, $r_s = 0.5\,\Omega$, $R_L = 20\,\Omega$, $D = 0.2$)

$$Z_S = r_S + j\omega L_S + \frac{R_L}{D^2} // \frac{1}{j\omega C_S}.$$

As shown in Fig. 9, the power output capability is much lower under high *k*. This result occurs because the value of $\mathrm{Re}Z_r$ is very large under high *k*, and the load amplification further enlarges $\mathrm{Re}Z_r$, resulting in a lower input current and input power. However, the load amplification can compensate for the decrease in $\mathrm{Re}Z_r$ under low *k*. Therefore, circuit has better energy transmission capacity under low *k*. The higher the output power is, the stronger the energy transmission capability of the circuit and the lower the requirement for the input voltage, thus reducing the requirement of the device and the cost of the system.

The efficiencies of different *k* are also shown in Fig. 9. From this figure, we can see that under low *k*, because the load amplification counteracts the efficiency decline caused by $\mathrm{Re}Z_r$ reduction, circuit has a higher efficiency.

B. Control Research of System Under Different Coupling

From the analysis in the previous section, we know that the circuit has greater power output and efficiency under specific parameters. However, if the system is required to have good circuit characteristics under any charging range, it is necessary to accurately control the circuit. The control variables of the system are mainly the duty cycle, the input voltage, and the input frequency. The influence of the input voltage on the system characteristics is simple, and the analysis is relatively simple. Therefore, we will mainly analyze the influence of D and the frequency on the system characteristics.

Formula (14) shows that $\mathrm{Re}Z_r$ varies with the square of D, and $\mathrm{Re}Z_r$ determines the output power and efficiency; thus, the control of D plays a decisive role in the system characteristics. We first analyze the effect of D on the output power of the system. The effect of different D on the output power under different *k* is shown in Fig. 10(a). This figure shows that the output power decreases with the decrease in D under high *k*, which indicates that D must be kept at a higher value to satisfy the output power of the system under high *k*. But this is not absolute. When the required power is not high, D could be small. In addition, the output power under low *k* is better than that

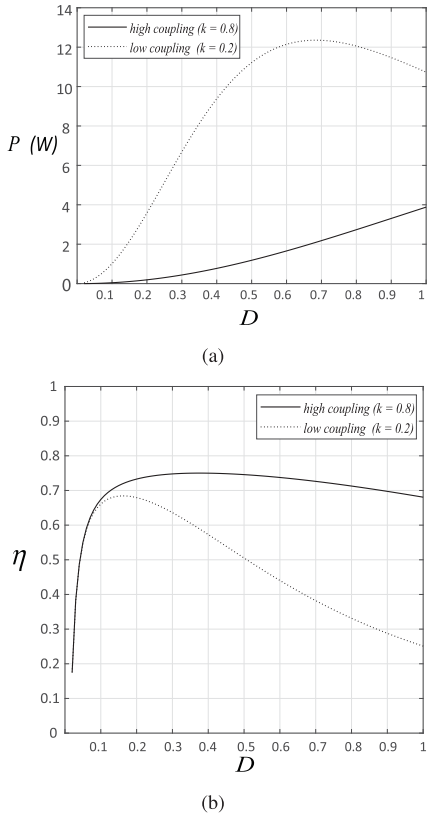

Fig. 10. Effect of D on the system under different k. (a) Output power. (b) Efficiency. ($L_P = 7.4\,\mu H$, $L_S = 25\,\mu H$, $C_P = 330\,nF$, $C_S = 47\,nF$, $r_p = 0.5\,\Omega$, $r_s = 0.5\,\Omega$, $R_L = 20\,\Omega$)

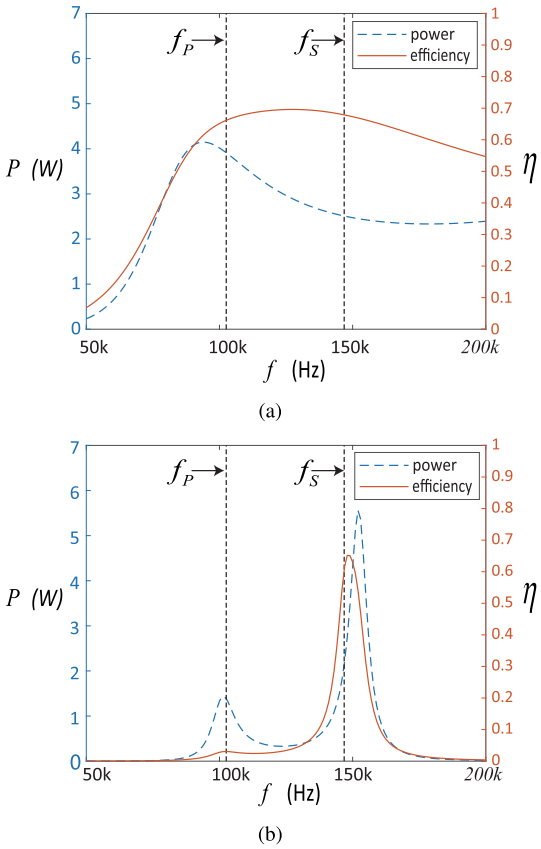

Fig. 11. Effect of f on the system under different coupling. (a) Under high coupling. (b) Under low coupling. ($L_P = 7.4\,\mu H$, $L_S = 25\,\mu H$, $C_P = 330\,nF$, $C_S = 47\,nF$, $r_p = 0.5\,\Omega$, $r_s = 0.5\,\Omega$, $R_L = 20\,\Omega$)

under high k, and the system can easily meet the requirements of output power. Therefore, compared with the high k, the system has a high power output capacity under low k, so unless in some extreme cases, the effect of D control on output power is not considered basically, because most D can meet the power requirements under low coupling.

The effect of different D on the efficiency under different k is shown in Fig. 10(b). This figure shows that when D is less than 0.1, the efficiency decreases significantly because the buck circuit loss increases sharply. When D is greater than 0.1, the overall efficiency under low k is worse than that under high k. In addition, the system efficiency does not change significantly with increasing D under high k, but the output power decreases rapidly with increasing D under low k. This result shows that the value of D has little effect on the efficiency under high k, but it must be kept at a low value to ensure the efficiency of the system under low k.

Through the abovementioned analysis, we can summarize the control methods of D: when k is high, the effect of D on the efficiency is not very large, and to ensure the power output, D must be at a relatively high value. When k is low, the system has enough output power, but to ensure efficiency, D must be at a low value.

As another control variable for the system, the change in input frequency destroys the resonant state of the circuit and changes the circuit characteristics of the system. Thus, the control of the input frequency also determines the quality of the system characteristics. According to the previous analysis, the resonant frequency f_P ($f_P = 1\sqrt{L_P C_P}$) of the transmitter is different from the resonant frequency f_S ($f_S = 1\sqrt{L_S C_S}$) of the receiver. In this article, the control method of the input frequency is designed by analyzing the different circuit characteristics when the input frequency is near f_P and near f_S.

The variation in output power and efficiency at different input frequencies under high k is shown in Fig. 11(a). This figure shows that an input frequency between f_P and f_S has little effect on the system efficiency. For the output power of the system, when the frequency is close to f_P, the output power of system is greatly improved. This result occurs because $\mathrm{Re}Z_r$ at f_P is lower than that at f_S, and thus, the input current at f_P is larger. Thus, the system has good power output characteristics under high k when the control frequency is close to f_P.

For low k, the output power and efficiency at different input frequencies are shown in Fig. 11(b). This diagram shows that the system has the highest efficiency and maximum output power when the input frequency is near f_S. This result occurs because $\mathrm{Re}Z_r$ at low k is generally small. When the control frequency is equal to f_S, the receiver is in the resonance state, and $\mathrm{Re}Z_r$ has the maximum value. Therefore, the system at f_S has good output characteristics and efficiency. Since the factors such as buck loss and coil resistance are added to the simulation, the

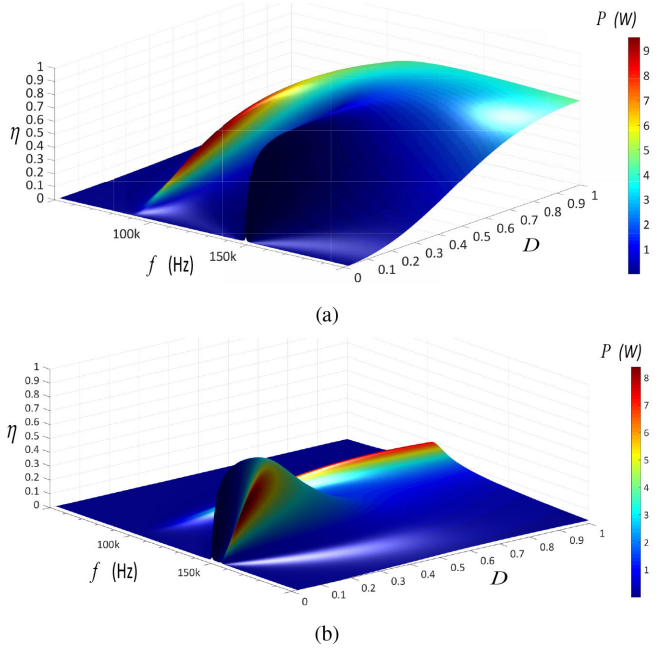

Fig. 12. Full view of the effects of D and f on system characteristics. (a) Under high coupling. (b) Under low coupling.

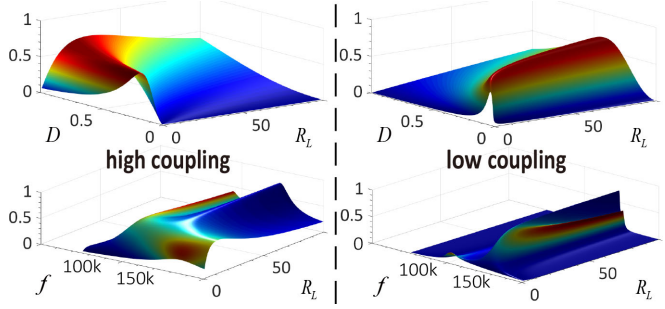

Fig. 13. Effect of load variation on system characteristics under different parameters.

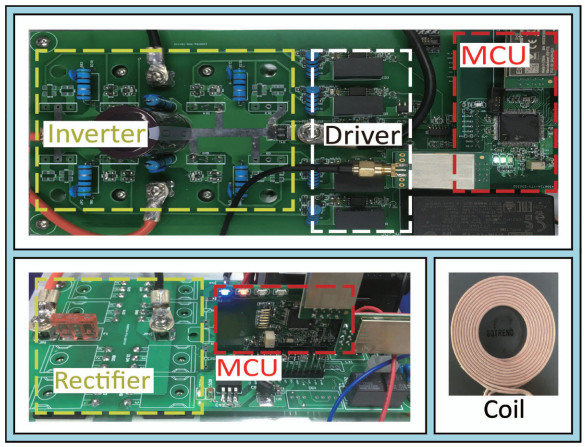

Fig. 14. System circuit.

frequency point of maximum power and efficiency shown in Fig. 11, is slightly different from f_S, but this effect will not impact the results analysis.

Through the abovementioned analysis, we can summarize the control method of the input frequency: when k is high, the frequency does not have a great impact on efficiency, and to meet the output power requirements, the input frequency should be close to f_p. When k is low, the system has the best output power and efficiency when the input frequency is close to f_s. The duty cycle D and frequency f jointly affect output power and system efficiency. One dimension plots in Figs. 10 and 11, only present limited profiles rather than a full view of the joint effect. Therefore, this paper draws the multidimensional Fig. 12, which intuitively shows the control range that can meet the system requirements under different coupling. It can be seen from Fig. 12(a) that the efficiency curve under high coupling is "plump", but only one area of output power has deep color, which means that the system can easily meet the needs of efficiency under high coupling, but there are few control inputs to meet the needs of power. It can be seen from Fig. 12(b) that the efficiency curve under low coupling is "slim", and there are two areas of output power with deep color, which means that the system can easily meet the needs of power under low coupling, but there are few control inputs to meet the needs of efficiency. In conclusion, the control of the system under high coupling should meet the power needs first and then the efficiency needs, while the control under low coupling is the opposite.

The effect of load resistance varies in most WPT applications, so Fig. 13 shows the effect of load variation on system characteristics under different parameters, where efficiency is ordinate and power is represented by color. From the two subfigures on the left, we can see that the system can easily achieve sufficient efficiency and power by adjusting D and f under high coupling and small R_L. However, when R_L is large, there is no area on the subfigures to meet the system efficiency and power requirements at the same time, which means that the system is difficult to meet the control requirements of high R_L under high coupling. For the two subfigures on the right, it is easy for the system to find an area that satisfies both efficiency and power in a wide R_L range, which means that the system has a larger R_L range under low coupling.

In conclusion, the system has a larger R_L range under low coupling than that under high coupling. At the same time, it can be seen from Fig. 13, that when the load is very small, the system characteristics will decrease rapidly. This is because when R_L is very small, the D needs a lower value to satisfy the amplification requirement of the reflection impedance, and a lower D causes the buck loss to increase rapidly. Therefore, to ensure the circuit characteristics of the system R_L cannot be too small.

IV. Experimental

A. Experimental Configuration

In this article, a complete system is designed for experimental verification. The system includes a transmitter and receiver, and meets the Qi standard. The system circuit is shown in Fig. 14, and the system block diagram is shown in Fig. 15. The circuit

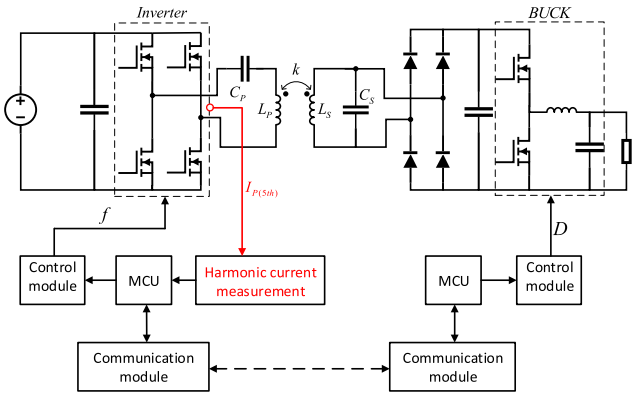

Fig. 15. Block diagram of the system.

TABLE III
CIRCUIT PARAMETERS

L_p (μH)	L_s (μH)	C_p (nF)	C_s (nF)	r_p (Ω)	r_s (Ω)	MOSFET
7.4	25	330	47	0.5	0.5	C2M0080
D_p (mm)	d_p (mm)	D_s (mm)	d_s (mm)	f_{IN} (KHz)	U_L (V)	BUCK
43	20	43	20	110-205	5	LM46002

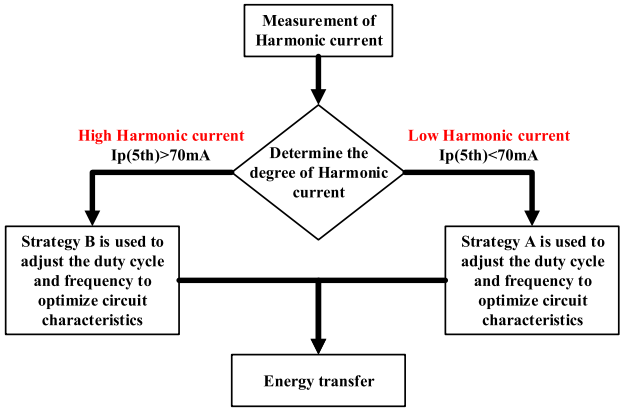

Fig. 16. System control flow.

parameters and some devices are shown in Table III. D_P and d_P are the outer and inner diameters of the transmitting coil, respectively, D_S and d_S are the outer and inner diameters of the receiving coil, respectively. The sizes of these coils also meet the Qi standard.

This article applies the control research of system in Section III to design the control flow, as shown in Fig. 16. The first step of the control process is to obtain the harmonic current for the design of the following control. The second step is to decide the next control strategy by judging the degree of harmonic current. When the system is under low harmonic current, control strategy A is adopted. Strategy A alleviates the efficiency reduction by reducing D while keeping the control frequency close to f_S to achieve efficiency and output power

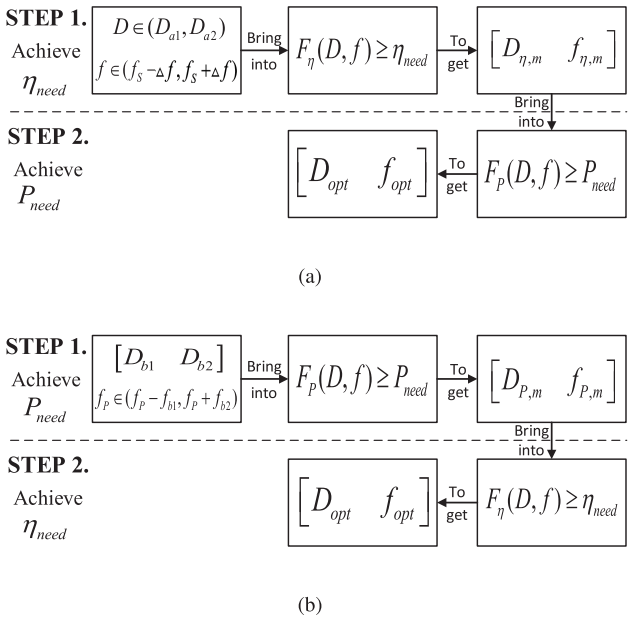

Fig. 17. Detailed process of system control. (a) Control strategy A. (b) Control strategy B.

optimization. When the system is under high harmonic current, control strategy B is adopted. Strategy B is to control D at a higher value and maintain the control frequency close to f_P to optimize the output power.

Corresponding to the control system shown in Fig. 16, Fig. 17 is a detailed process for realizing its control purpose. The control inputs of strategy A and B are duty cycle D and frequency f. Their purpose is to achieve the required output power P_{need} and required efficiency η_{need}. The mathematical expression is to solve the following formula:

$$\begin{cases} F_\eta(D,f) \geq \eta_{\text{need\_LowerBound}} \\ F_P(D,f) \geq P_{\text{need\_LowerBound}} \end{cases} \tag{17}$$

where $F_P(D,f)$ is the output power formula (16) and $F_\eta(D,f)$ is the system efficiency formula (15). According to the analysis in the aforementioned section, for strategy A with low coupling, there are more control inputs to achieve P_{need}, but less to meet η_{need}. Therefore, in order to reduce the operation cost, strategy A first brings the initial value into $F_\eta(D,f)$ to get the control input group $[D_{\eta,m} \ f_{\eta,m}]$ which can achieve η_{need} (m represents the number of control inputs), and then brings $[D_{\eta,m} \ f_{\eta,m}]$ into $F_P(D,f)$ to get the optimal control input $[D_{\text{optimal}} \ f_{\text{optimal}}]$.

The possible nonmonotonic relationship between duty-cycle and power in Fig. 10(a) may cause trouble for control, while achieving η_{need} first will reduce the probability of nonmonotonic relationship. This is because there are fewer control inputs to achieve η_{need} under low coupling, and the probability that they still have the same output power is especially lower. Furthermore, the smaller definition of the initial value of D can also reduce the probability of nonmonotonic relationship. This is also one of the important reasons why strategy A is designed in this article.

Fig. 17(a) shows the process of strategy A, where the initial values are defined according to the analysis in the previous section. The initial value D is defined to a relatively small value $D \in (D_{a1}, D_{a2})$, and the initial value f is defined near f_s [$f \in (f_S - \Delta f, f_S + \Delta f)$], where D_{a1} and D_{a2} are set to 0.1 and 0.4, and Δf set to 5 KHz. The specific initial value setting process requires a lot of data comparison and is not absolute, so this article will not further describe in detail.

For strategy B with high coupling, there are more control inputs to achieve η_{need}, but less to meet P_{need}. Therefore, for control strategy B, it is opposite to strategy A. It first brings the initial value into $F_P(D, f)$ to get the $[D_{P,m}\ f_{P,m}]$, which can achieve P_{need}, and then brings $[D_{P,m}\ f_{P,m}]$ into η_{need} to get $[D_{\text{optimal}}\ f_{\text{optimal}}]$. Fig. 17(b) shows the process of strategy B. The initial value D is defined to a relatively large value $D \in (D_{b1}, D_{b2})$, and the initial value f is defined near f_P [$f \in (f_P - f_{b1}, f_P + f_{b2})$], where D_{b1} and D_{b2} are set to 0.3 and 0.9, and f_{b1} and f_{b2} are set to 5 KHz and 40 KHz.

For the measurement of harmonic current, this article recommends two methods, the first is offline method. The measurement environment of offline method is when the system does not transmit power. The inverter outputs a square wave with the same harmonic frequency to simulate harmonic. At this time, the output current of the inverter is equal to the harmonic current. The advantage of this method is that the current rms can be measured directly without band-pass filter circuit. The second method to measure the harmonic current is online method, which measures the harmonic current when the system transmits power. The advantage of this method is that k can be estimated in real time, which is suitable for dynamic WPT system. Because this article does not need the function of dynamic real-time control, it adopts a simpler offline method.

B. Experimental Results

For experimental results, we first measure the harmonic current $I_{P(5th)}$ by offline method. $I_{P(5th)}$ measured at different charging distance is shown in Fig. 18(a). It can be seen from the figure that $I_{P(5th)}$ decreases rapidly as the distance increases. At the same time, when the distance is close, the inductance will be increased due to the influence of ferrite between the coils, which will lead to the increase of $I_{P(5th)}$. Therefore, Fig. 18(a) shows two kinds of simulation data, with and without inductance correction, in which the curve with correction is closer to the measurement curve. The waveform measured by the offline method is shown in Fig. 18(b). In order to show the waveform more clearly, the input voltage of the inverter is appropriately increased on the figure.

Fig. 19 shows the efficiency η ($\eta = P_L\ P_{\text{Inverter}}$) and power transfer capability G_V ($G_V = V_L\ V_{\text{Inverter}}$) of the system at different distances, where P_{Inverter} is the input power of the inverter and V_{Inverter} is the input voltage of the inverter. The experimental results show that the average efficiency of the system can be maintained above 70% when the charging distance is less than 5 mm and at 60% when the distance is 20 mm, while in the same case, the efficiency of the Qi standard is only 28%. At the same time, it is noted that the efficiency is lower than Qi at 2

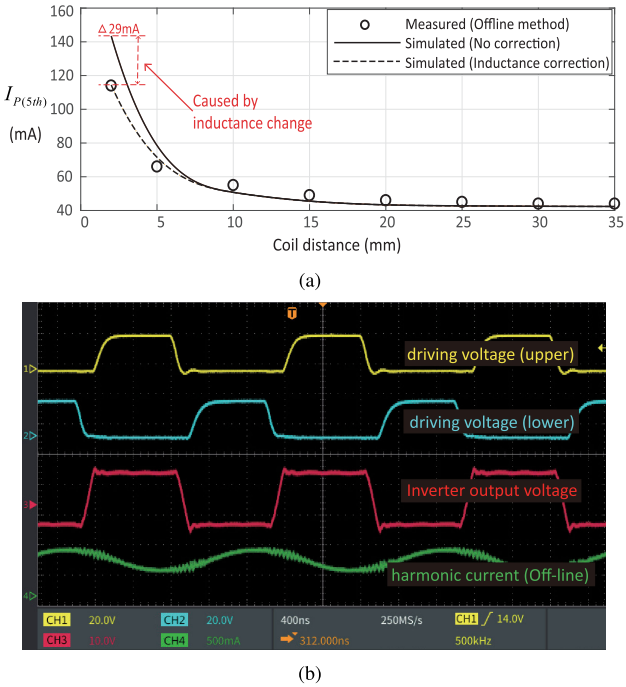

Fig. 18. (a) Harmonic current at different charging distances. (b) Measurement of harmonic current waveform by offline method.

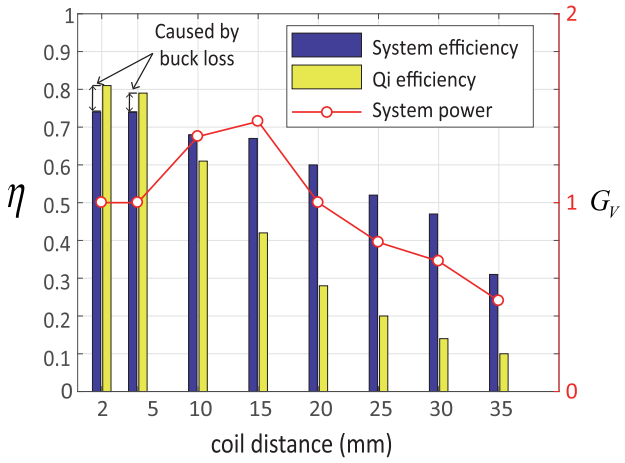

Fig. 19. Efficiency and output power in the experiment.

and 5 mm, this is because Qi controls the inverter according to the required power, and there is no special buck control method [19]. Therefore, Qi's experimental circuit has no buck circuit, so Qi has no buck loss, which leads to Qi's higher efficiency under low charging distance.

For the power transmission capacity, the G_V can be maintained previously 1 in the distance of 20 mm. G_V reaches its maximum value near 15 mm and then decreases with increasing distance.

Table IV shows the circuit parameters in the experiment. This table shows that when the system is in low harmonic current, the input frequency is close to f_S, and D is low. When the system

TABLE IV
SYSTEM PARAMETERS IN THE EXPERIMENT

Coil spacing (mm)	$I_{P(5th)}$ (mA)	Inverter frequency (KHz)	inverter current (A)	buck voltage (V)	Duty cycle
2	114	107	0.34	12	0.42
5	66	130	0.34	15	0.33
10	55	135	0.5	13	0.38
15	49	150	0.53	22	0.23
20	46	147	0.42	23	0.22
30	44	147	0.37	30	0.17

is in high harmonic current, the input frequency of the system is close to f_P, and D is relatively high.

The Qi standard has a fixed output voltage and a variable output current, and thus, the load resistance R_L is variable. We have also experimented with different R_L. The experimental results show that when $R_L > 10\,\Omega$, the system characteristics do not change much, but when $R_L < 10\,\Omega$, the experimental results show that the efficiency is significantly reduced under low harmonic current. This is consistent with the abovementioned analysis.

The control system in this article is compared with Qi standard, which employs feedback control to maintain target output voltage or current at varying load and coupling factor conditions. However, according to the block diagram in Fig. 17, the controller in this article adopts a feedforward rather than a feedback control strategy. The feedforward control means that the optimal control input $[D_{\text{optimal}}\ f_{\text{optimal}}]$ are obtained from system formula (17), instead of from error signal in the feedback paradigm. Therefore, this article can not maintain constant output at varying load and coupling factor conditions. Feedforward is used because the main purpose of this article is to highlight that the control system has the function of estimating *k*, rather than comparing the control performance with Qi. At the same time, the future research of this article is the application of the proposed method at varying load and coupling factor conditions.

V. CONCLUSION

As the key parameter of the WPT system, the estimation of the coupling coefficient *k* is very important. The traditional method of estimating *k* is mainly to measure and calculate the electrical signal generated by fundamental. However, the characteristics of the WPT system under the fundamental frequency are resonance nonlinear, which has a very complex relationship with *k*. It requires many parameters and complex calculations to estimate *k* by analyzing these electrical signals, which makes the traditional method of estimating *k* difficult to have good robustness and application in practice.

The WPT circuit can be simplified in high frequency, and the input square wave of the system contains high frequency harmonics. Thus, this article proposes a method of estimating *k* only by the harmonic current. By comparing formula (7) with formulas (1) and (3), it can be found that for the method proposed in this article, only one electrical signal $L_{P(5th)}$ and three circuit parameters U_{IN}, ω and L_P are needed to estimate *k*, which greatly reduces the process of estimating *k* by simplifying the circuit in high frequency. To show the contribution points of this method more intuitively, Tables I and II summarize the methods for estimating *k* and focus on the differences in the amount of calculations and robustness.

According to the method proposed in this article, a wide charging range WPT control system is designed. For the control research of system, this article mainly researches the influence of the duty cycle and input frequency. After analyzing the influence of different control parameters on the system under different *k*, the control methods of D and the input frequency under high *k* and low *k* are obtained, respectively.

This article designs an system that meets the Qi standard to carry out experimental verification. The system efficiency can be maintained previously 70% when the charging distance is less than 5 mm and 60% when the charging distance is 20 mm. The experimental results show that the original 10 mm Qi standard charging distance can reach 20 mm.

REFERENCES

[1] Z. Zhang, H. L. Pang, A. Georgiadis, and C. Cecati, "Wireless power transfer-an overview," *IEEE Trans. Ind. Electron.*, vol. 66, no. 2, pp. 1044–1058, Feb. 2019.

[2] J. L. Zhou, B. Zhang, W. X. Xiao, D. Y. Qiu, and Y. F. Chen, "Nonlinear parity-time-symmetric model for constant efficiency wireless power transfer: Application to a drone-in-flight wireless charging platform," *IEEE Trans. Ind. Electron.*, vol. 66, no. 5, pp. 4097–4107, May 2019.

[3] H. C. Li, K. P. Wang, J. Y. Fang, and Y. Tang, "Pulse density modulated ZVS full-bridge converters for wireless power transfer systems," *IEEE Trans. Power Electron.*, vol. 34, no. 1, pp. 369–377, Jan. 2019.

[4] Y. M. Zhang, T. Z. Kan, Z. C. Yan, Y. H. Mao, Z. X. Wu, and C. C. Mi, "Modeling and analysis of series-none compensation for wireless power transfer systems with a strong coupling," *IEEE Trans. Power Electron.*, vol. 34, no. 2, pp. 1209–1215, Feb. 2019.

[5] Z. C. Yan *et al.*, "Frequency optimization of a loosely coupled underwater wireless power transfer system considering eddy current loss," *IEEE Trans. Ind. Electron.*, vol. 66, no. 5, pp. 3468–3476, May 2019.

[6] J. Hu and J. Zhao, "Design of wireless power transfer system with input filter," *IET Power Electron.*, vol. 13, no. 7, pp. 1393–1402, May 2020.

[7] A. Moradi, F. Tahami, and M. A. GhaziMoghadam, "Wireless power transfer using selected harmonic resonance mode," *IEEE Trans. Transp. Electrif.*, vol. 3, no. 2, pp. 508–519, Jun. 2017.

[8] H. L. Zeng, S. T. Yang, and F. Z. Peng, "Design consideration and comparison of wireless power transfer via harmonic current for PHEV and EV wireless charging," *IEEE Trans. Power Electron.*, vol. 32, no. 8, pp. 5943–5952, Aug. 2017.

[9] H.-S. Jang, J.-W. Yu, and W.-S. Lee, "1-port measurement method of the coupling factor and receiver for spatial and state freedom in wireless power transfer systems," *IEEE Trans. Antennas Propag.*, vol. 64, no. 9, pp. 4098–4102, Sep. 2016.

[10] J. Yin, D. Lin, T. Parisini, and S. Y. Hui, "Front-End monitoring of the mutual inductance and load resistance in a series–series compensated wireless power transfer system," *IEEE Trans. Power Electron.*, vol. 31, no. 10, pp. 7339–7352, Oct. 2016.

[11] J. P.-W. Chow, H. S.-H. Chung, and C.-S. Cheng, "Use of transmitter-side electrical information to estimate mutual inductance and regulate receiver-side power in eireless inductive link," *IEEE Trans. Power Electron.*, vol. 31, no. 9, pp. 6079–6091, Sep. 2016.

[12] D. Yang, S. Won, J. Tian, Z. Cheng, and J. Kim, "A method of estimating mutual inductance and load resistance using harmonic components in wireless power transfer system," *Energies*, vol. 12, no. 14, pp. 2728–2747, Jul. 2019.

[13] K. Hata, T. Imura, and Y. Hori, "Efficiency maximization of wireless power transfer based on simultaneous estimation of primary voltage and mutual inductance using secondary-side information," in *Proc. 42nd Annu. Conf. IEEE Ind. Electron. Soc., Florence*, 2016, pp. 4487–4492.

[14] D. Kobayashi, T. Imura, and Y. Hori, "Real-time coupling coefficient estimation and maximum efficiency control on dynamic wireless power transfer for electric vehicles," in *Proc. IEEE PELS Workshop Emerg. Technol. Wireless Power*, 2015, pp. 1–6.
[15] G. Lovison, T. Imura, and Y. Hon, "Secondary-side-only simultaneous power and efficiency control by online mutual inductance estimation for dynamic wireless power transfer," in *Proc. 42nd Annu. Conf. IEEE Ind. Electron. Soc., Florence*, 2016, pp. 4553–4558.
[16] R. Jin, Z. P. Yang, and F. Lin, "Mutual inductance identification and maximum efficiency control of wireless power transfer system for the modern tram," in *Proc. IEEE PELS Workshop Emerg. Technol. Wireless Power Transfer*, 2017, pp. 70–74.
[17] X. Dai, X. F. Li, Y. L. Li, and A. G. P. Hu, "Maximum efficiency tracking for wireless power transfer systems with dynamic coupling coefficient estimation," *IEEE Trans. Power Electron.*, vol. 33, no. 6, pp. 5005–5015, Jun. 2018.
[18] V. Jiwariyavej, T. Imura, and Y. Hori, "Coupling coefficients estimation of wireless power transfer system via magnetic resonance coupling using information from either side of the system," *IEEE J. Emerg. Sel. Top. Power Electron.*, vol. 3, no. 1, pp. 191–200, Mar. 2015.
[19] D. van Wageningen and T. Staring, "The Qi wireless power standard," in *Proc. 14th Int. Power Electron. Motion Control Conf.* 2010, pp. S15-25–S15-32.
[20] C. L. Wei, C. H. Chen, K. C. Wu, and I. T. Ko, "Design of an average-current-mode noninverting buck-boost DC-DC converter with reduced switching and conduction losses," *IEEE Trans. Power Electron.*, vol. 27, no. 12, pp. 4934–4943, Dec. 2012.

Jianghao Hu was born in China, in 1991. He received the B.S. and M.S. degrees in control science and engineering from the Dong Hua University, Shanghai, China, in 2013 and 2016, respectively. He is currently working toward the Ph.D. degree in instrument science and engineering with the Shanghai Jiao Tong University, Shanghai, China.

His current research interests include wireless power transfer and power electronics.

Jiankang Zhao received the Ph.D. degree from the National University of Defense Technology, Changsha, China, in 2006.

He is currently a Professor with the School of Electronic Information and Electrical Engineering, Shanghai Jiao Tong University. His research interests include aircraft navigation and system control.

Chao Cui received the B.S. degree in control technology and instruments from Chongqing University, Chongqing, China, in 2015. He is currently working toward the Ph.D. degree with the Shanghai Jiao Tong University, Shanghai, China.

His research interests include state estimation, computer vision, and sensor fusion for low-cost aerial robots in complex environments.